Journal of Fluids and Structures (1999) **13,** 853–864
Article No.: jfls. 1999.0241, available online at http://www.idealibrary.com on IDEAL®

SOME EXPERIMENTS ON FLOW-INDUCED VIBRATION OF A CIRCULAR CYLINDER WITH SURFACE ROUGHNESS

A. Okajima, T. Nagamori, F. Matsunaga, T. Kiwata

Department of Mechanical Systems Engineering, Kanazawa University
Kodatsuno 2-40-20, Kanazawa, 920-8667 Japan

(Received 22 October 1998 and in revised form 29 July 1999)

Aeroelastic instability of a circular cylinder with surface roughness was experimentally studied by free-oscillation tests in a wind tunnel. Flows at high Reynolds numbers could be simulated at relatively low wind velocities, by introducing surface roughness, so as to reduce the value of the critical Reynolds number. The response amplitudes of a roughened cylinder oscillating in the transverse (cross-flow) direction in the flow were measured. The measured range of reduced velocity is about 1·5–8, which includes the critical velocity. The value of a reduced mass-damping parameter (the Scruton number) is constant at about 6. For the aeroelastic instability in the transverse direction, it was found that the oscillation of the roughened cylinder induced by a vortex-excitation is damped down in a small velocity range covering the critical Reynolds number. At Reynolds numbers higher than the critical value, a roughened cylinder vibrates with a large amplitude again, associated with a lock-in phenomenon due to the coincidence of the wake-frequency and the natural frequency of the oscillating cylinder.

© 1999 Academic Press

1. INTRODUCTION

From the practical engineering point of view, flow-induced vibrations of a circular cylinder have been of great interest for many decades. It has long been known that vortex shedding can induce an elastically supported cylinder to vibrate with a large amplitude. Examples of damage on a circular structure caused by flow-induced vibrations are by no means rare. For example, the damage of a thermocouple occurred in the fast breeder reactor "Monju" of the Japan Nuclear Cycle Development Institute in 1995 was caused mainly by a streamwise flow-induced vibration since the structural damping of the thermocouple was extremely small and its natural frequency was very near to twice the critical frequency of flow-induced vibration. In addition, it is noted that this vibration of a thermocouple occurred in flow with a high turbulence intensity, at a high Reynolds number, over 10^5.

Vortex shedding from an elastically supported cylinder can cause the cylinder to oscillate in the transverse (cross-flow) and streamwise (in-line) directions. However, when the cylinder has a certain structural damping and the mass-ratio is large, such as in the air, it is more usual to obtain oscillation in the transverse direction than in the streamwise one. Free-oscillation tests of a circular cylinder in the transverse direction were conducted by many researchers, e.g., by Scruton (1963), Feng (1968), Wootton (1969), Brika & Laneville (1994), and so on. While the largest part of research efforts have been focused on transverse vibration, there are some studies on the streamwise vibration of circular cylinder in the subcritical regime below the critical Reynolds number. For example, King, Prosser & Johns (1973) carried out experiments on streamwise vibration of a flexible cantilevered beam of circular cylinder in a water channel.

0889–9746/99/100853 + 12 $30.00 © 1999 Academic Press

Many studies of free-oscillation tests of smooth circular cylinders, however, have been limited to the subcritical flow regime, below the critical Reynolds number, except for the studies by Wootton (1969), who carried out experiments on the cylinders with smooth and roughened surfaces at high Reynolds numbers.

It is difficult to carry out free-oscillation tests at Reynolds numbers higher than the critical Reynolds number, because it is not easy to have a very high natural frequency of oscillation of the cylinder and also the test wind velocity cannot be increased too much, since the critical reduced velocity (the nondimensional onset velocity of the vortex-excited oscillation) is fixed. So, in order to simulate the flow in the range of Reynolds numbers higher than the critical one at relatively low test wind velocities, a circular cylinder with surface roughness is used in wind tunnel tests.

Three kinds of evenly roughened surfaces were adopted, as described in Section 2.2. The value of the critical velocity (the threshold velocity) was varied by changing the natural frequency of the oscillating cylinder system, and thus the Reynolds number range of the vortex-excited oscillation was changed. Hence, the aeroelastic instability of a roughened cylinder can be studied by the free oscillation test method in the Reynolds number range near and higher than the critical Reynolds number.

2. WIND-TUNNEL EXPERIMENTS

2.1. Wind-Tunnel Facilities

Measurements were made by mounting a model of a circular cylinder on a working section of 0·3 m × 1·2 m of an open typed low-speed wind-tunnel, as shown in Figure 1. The range of wind velocity was $U = 1$–30 m/s. The turbulence intensity level of the uniform flow in the working section was less than about 0·5%.

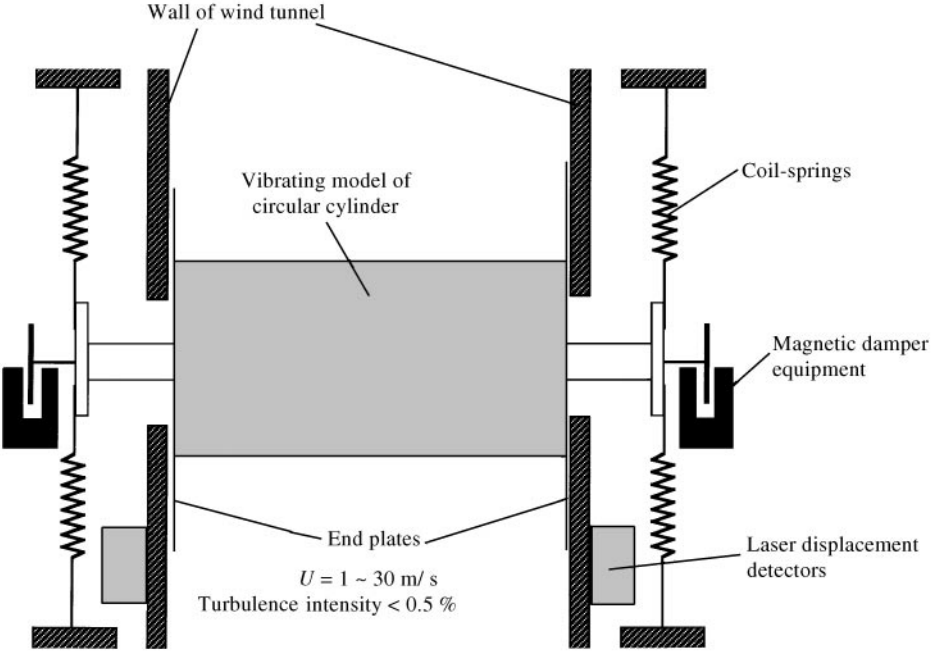

Figure 1. Measurement section of an open type low-speed wind-tunnel.

2.2. Models of Cylinder with Surface Roughness

The test models had a diameter of $D = 160$ mm, and a span of 293 mm; they were made of acrylic acid resin. Unfortunately, the aspect ratio of this cylinder was small, about 1·8, and the blockage ratio was large, about 13·8% in the working section of the wind tunnel. The present data of static drag coefficient C_D were corrected for blockage effects according to the procedure of Allen & Vincenti (1944). The models of a circular cylinder were covered with different surface roughness. In the present experiment, three kinds of evenly roughened surfaces were adopted; two of them had the roughness uniformly distributed by spherical glass bead particles of a diameter d of about 0·8 mm ($d/D = 5{\cdot}0 \times 10^{-3}$) and 1·0 mm ($d/D = 6{\cdot}2 \times 10^{-3}$), respectively, and the third roughness was made by attaching to the surface 64 stranded cables with a diameter of 6 mm. The cross-sectional views of the surface appear undulated, as shown in Figure 2. The strands were stuck to the cylinder surface, twisted with a pitch of $11{\cdot}5D$ in the spanwise direction.

An oscillating cylinder model was suspended by an arrangement of wires and coil-springs to vibrate freely in the transverse direction. There were narrow gaps of about 1–2 mm between the walls of wind-tunnel and the end-plates of the model. The natural frequency f of the oscillating cylinder system was changed in the range of 4·20–7·15 Hz by replacing the sets of coil-springs with others with different values of natural frequencies. Thus the values of Reynolds number, UD/ν, where ν is the kinematic viscosity, and U a wind velocity during a free-oscillation tests, were able to change in the range of $\mathrm{Re} = UD/\nu = 1{\cdot}5 \times 10^4$–$1{\cdot}1 \times 10^5$, including the critical Reynolds number of each roughened cylinder. The logarithmic damping decrement of the oscillating system of the cylinder was calculated from the decay of displacement amplitudes during free oscillation in still air. This leads to the reduced mass-damping parameter, or Scruton number, $\mathrm{Sc} = 2M\delta/\rho D^2 L$, where M is the equivalent mass of the oscillating system, ρ the fluid density and L the span-length of the cylinder. The value of the reduced mass-damping parameter, Sc was kept at about 6, by controlling the magnetic damper equipment installed at the ends of the oscillating test model outside the wind tunnel, as shown in Figure 1. The values of the diameter of a circular cylinder D, the natural frequency f, equivalent mass M, the logarithmic damping decrement δ, the mass ratio $M/\rho D^2 L$, and the reduced mass-damping parameter Sc of the oscillating test-models used are summarized in Tables 1–3 for the cylinders with the three kinds of surface roughness. The amplitudes a_y of the oscillating cylinder in the transverse direction were measured by a laser displacement detector and reduced to a nondimensional response amplitude, $\eta = a_y/D$. The frequency f_w of the fluctuation velocity in the wake was detected by a hot-wire probe which was inserted at the position of $0{\cdot}5D$ above and $2D$ downstream from the center of a cylinder, and analyzed by the PC.

3. EXPERIMENTAL RESULTS AND DISCUSSION

3.1. Static Characteristics of a Stationary Circular Cylinder with Surface Roughness

Figure 3 shows the static aerodynamic characteristics of a stationary circular cylinder, i.e., the drag coefficient C_D and the Strouhal number St of the cylinders with the different types of surface roughness compared with the results of a smooth cylinder. The measured range of Reynolds numbers is from $2{\cdot}5 \times 10^4$ to $3{\cdot}2 \times 10^5$. From this figure, it can be seen that the flow region covering the critical Reynolds number lies between $\mathrm{Re} = 5 \times 10^4$ and 6×10^4 for the cylinders roughened with stranded cables of a diameter of 6 mm and glass beads of a diameter of 1 mm, and at $\mathrm{Re} = 7{\cdot}8 \times 10^4$–$8{\cdot}3 \times 10^4$ for the cylinder roughened with glass

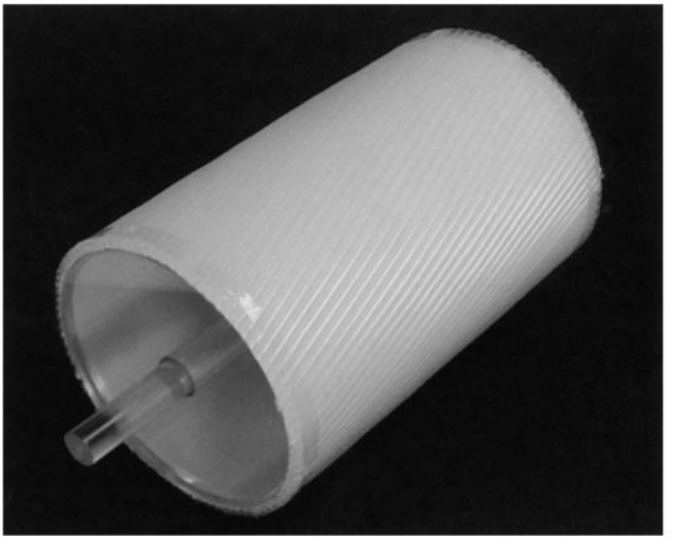

$D = 177$ mm, $d = 6$ mm, $d/D = 0.034$

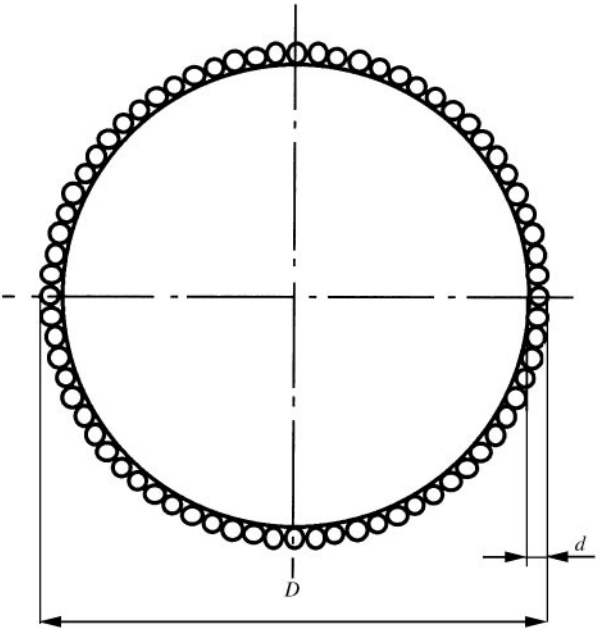

Figure 2. A test model of a circular cylinder with surface roughness consisting of 64 stranded cables of 6 mm diameter.

beads of a diameter of 0·8 mm, where the drag coefficient reduces to a minimum value of about 0·6.

The alternate vortex-shedding, like a Karman vortex-street, seems to disappear in these ranges, as a frequency component with a very sharp peak cannot be detected from the spectra of fluctuating velocities in the wake. The flow region corresponding to the critical Reynolds number is successfully simulated around relatively low values of wind velocity,

TABLE 1

Parameters of the test model, with surface roughness produced by stranded cables of 6 mm in diameter.

D m	0·177			
f Hz	4·2	5·5	5·95	7·15
M kg	1·94	1·91	1·89	1·92
δ	0·0171	0·0172	0·0178	0·0172
$M/\rho D^2 L$	175	173	172	174
Sc	6			

TABLE 2

Parameters of the test model, with surface roughness produced by glass beads of 1 mm in diameter

D m	0·167			
f Hz	4·10	5·85	7·08	8·88
M kg	1·79	1·93	1·94	1·94
δ	0·0160	0·0148	0·0147	0·0147
$M/\rho D^2 L$	188	202	204	204
Sc	6			

TABLE 3

Parameters of the test model, with surface roughness produced by glass beads of 0·8 mm in diameter

D m	0·167		
f Hz	7·38	7·82	9·28
M kg	1·80	1·78	1·79
δ	0·0160	0·0161	0·0159
$M/\rho D^2 L$	188	186	188
Sc	6		

$U = 4{\cdot}5$ and 7 m/s, respectively, by employing the cylinders with the roughened surface. With increasing Reynolds number, reaching over 7×10^4 and $1{\cdot}1 \times 10^5$, the drag coefficient gradually recovers and reaches $C_D = 0{\cdot}9$–$1{\cdot}0$, and the periodic vortex shedding with relatively high values of Strouhal number, $\mathrm{St} = 0{\cdot}24$–$0{\cdot}27$ comes back. It can be seen in Figure 3 that flows near and higher than the critical Reynolds number can be achieved at relatively small values of wind velocity. The free-oscillation tests at such low values of wind velocity can be done in the present experimental facilities.

3.2. Response Characteristics of Transverse Oscillation

Figure 4(a) shows the r.m.s. values of the free response amplitudes, $\eta = a_y/D$, of transverse oscillation for a cylinder roughened with stranded cables against the reduced velocity

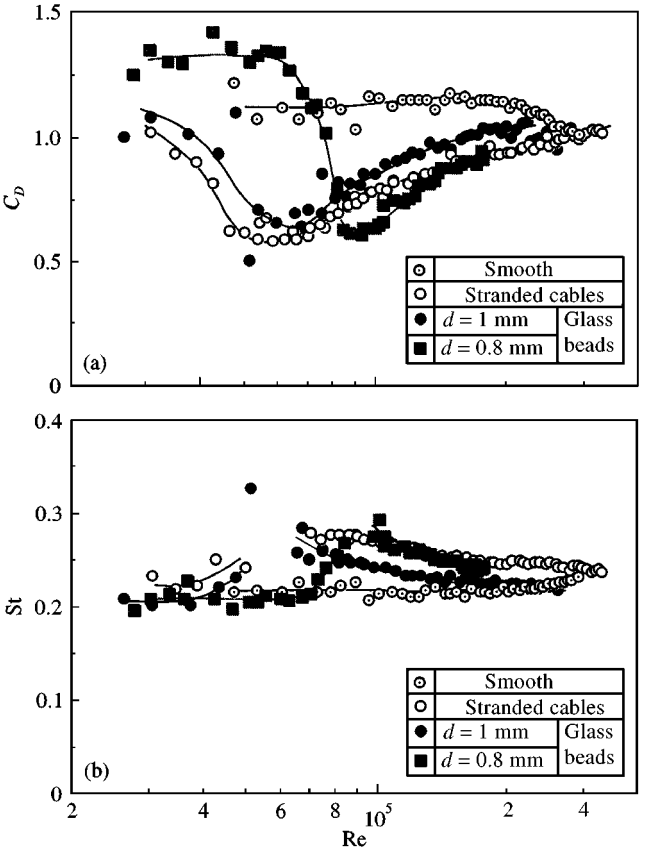

Figure 3. Static aerodynamic characteristics of a stationary circular cylinder, roughened with different types of the surface roughness: (a) Drag coefficient C_D; (b) Strouhal number St.

$\bar{U}(= U/fD)$. The four curves correspond to different values of the natural oscillation frequency f from 4·20 to 7·15 Hz of the cylinder. The response amplitude η abruptly increases at each different onset velocity, that is, the critical velocity. It is usual for the corresponding response amplitudes to fall onto the same curve of nondimensional amplitude η versus the reduced velocity $\bar{U}$, because the reduced mass-damping parameter Sc of all free-oscillation tests is kept constant at about 6, when the oscillation tests of cylinder with different natural frequencies are carried out in the subcritical regime. However, it is apparent from the results in Figure 4 that the critical values of the reduced onset velocity of oscillation and the aeroelastic unstable ranges are quite different for each test, i.e., for the various natural frequencies. The strange shape of response curves with two peaks can be found in the response curve of the test cylinder with a natural frequency of $f = 9{\cdot}28$ Hz in Figure 4(b) for the cylinder roughened with glass beads of a diameter of 0·8 mm. The effect of Reynolds number appears distinctly on the response curves of the roughened cylinders as the test flows are around the critical Reynolds number.

Next, the response amplitudes η of transverse oscillation of the cylinders roughened by stranded cables are plotted against the Reynolds number Re in Figure 5, together with the results of Strouhal number obtained from a fluctuating velocity in the wake. It can be inferred from the static characteristics of Figure 3 that unstable aeroelastic region for the cases with a natural frequency of 4·20 Hz belongs to the flow region below the critical

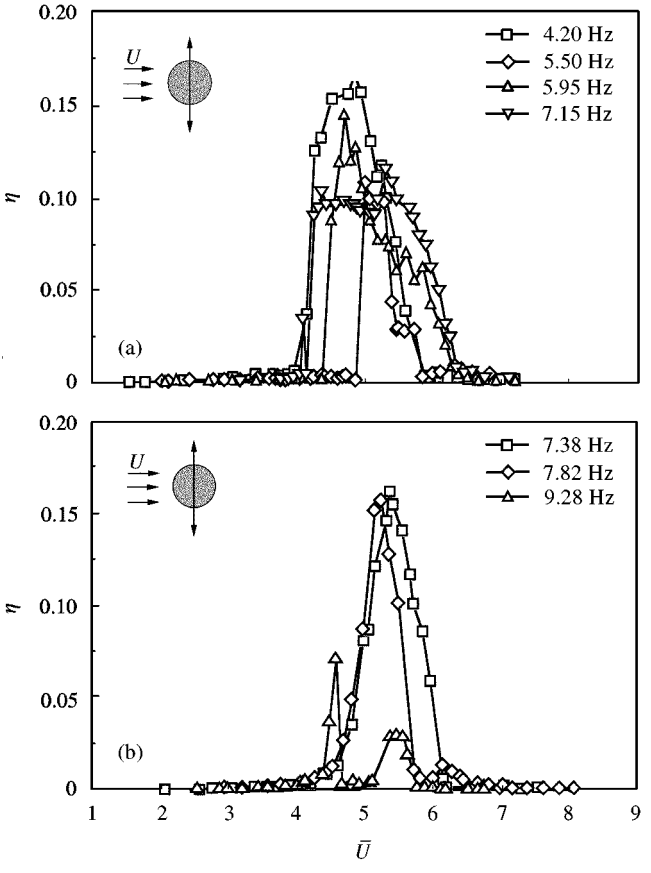

Figure 4. The r.m.s. values, $\eta = a_y/D$ of the displacement response amplitudes of the cylinders roughened with (a) stranded cables and (b) glass beads, versus the reduced velocity $\bar{U}$; the reduced mass-damping parameter corresponds to Sc = 6.

Reynolds number (the subcritical regime) in Figure 5(a, b) for the cylinder roughened with stranded cables. The maximum amplitude of this curve reaches $\eta \approx 0{\cdot}16$, which is in good agreement with the corresponding results of Scruton (1963) for the same value of a damping parameter. With an increase in the natural frequency of the cylinder from 5·5 to 7·15 Hz, the onset velocity becomes so high that the flow region of vortex excitation can include the flow near and over the critical Reynolds number. It is noted that in a narrow Reynolds number region around $\mathrm{Re} = 5 \times 10^4 - 6 \times 10^4$, all amplitude curves of the cylinder oscillation are diminished, being damped as shown in Figure 5(a), and the wake-flow is not locked-in, i.e., the values of Strouhal number increase to high values, up to 0·25–0·34, the same value as that of a stationary cylinder, as shown in Figure 5(b). This implies that the oscillation of the cylinder induced by vortex excitation is damped down by a small structural damping effect, i.e., the negative damping force is very weak, around the critical Reynolds number. So, when the natural frequencies are 5·5 and 5·95 Hz, the occurrence of vortex-excited oscillation is limited to a very narrow range over the critical Reynolds number.

Figure 6 shows the variation of spectra of velocity in the wake of the oscillating cylinders roughened by stranded cables, as compared with the response amplitude and the corresponding static curve of drag coefficient C_D. Referring to the static curve of C_D, it is deduced that the flow in Figure 6(a) is in the subcritical regime of this roughened cylinder; in (b) the

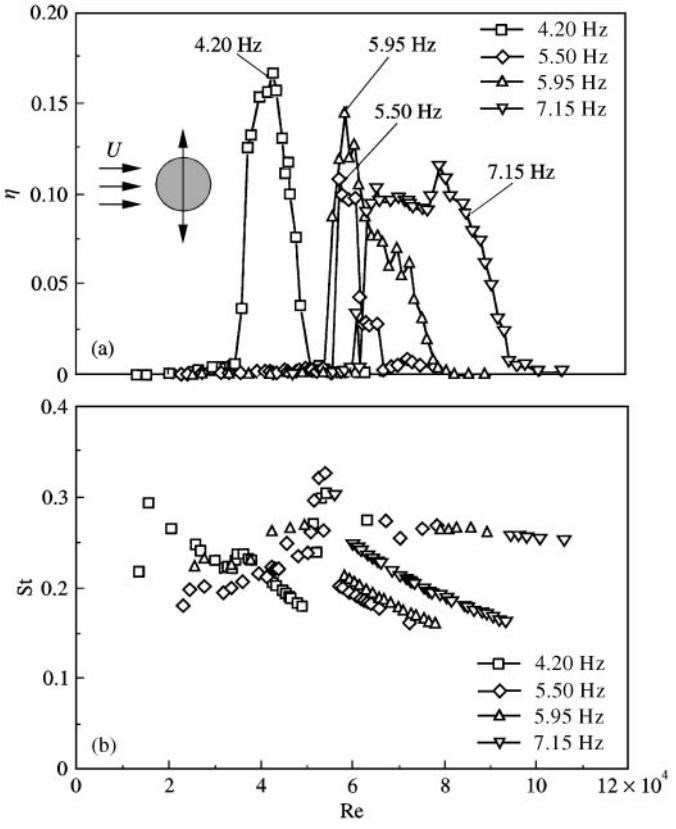

Figure 5. (a) The r.m.s. values, $\eta = a_y/D$ of the displacement response amplitudes, and (b) the Strouhal numbers St of the cylinder roughened with stranded cables against the Reynolds number Re, for Sc = 6.

flow is near the critical Reynolds number; and in (c) and (d) it is over the critical value. It should be noted that there is no discernible peak in the spectra of the flow in (b), which signals the disappearance of vortex shedding in this region, while sharp spectral peaks appear in the flow in the cases of (a), (c) and (d). The lock-in phenomenon is noted in the case of (c), where the wake frequency coincides with the frequency of the oscillating cylinder.

For the case of the highest natural frequency of 7·15 Hz in Figure 5, the wind velocity and the Reynolds number during the oscillation tests become relatively high. As the value of Strouhal number is 0·3 near the critical Reynolds number, and 0·25 over the critical one as in Figure 5(b), the corresponding values of the reduced critical velocity $\bar{U}_{cr}$ are 3·3 and 4; the corresponding Reynolds numbers can be estimated to be about $4{\cdot}7 \times 10^4$ and $5{\cdot}6 \times 10^4$, respectively. It is apparent from Figure 3(a) that the flow for $\bar{U}_{cr} = 3{\cdot}3$ is the region near the critical Reynolds number and that of $\bar{U}_{cr} = 4$ is over the critical one. This cylinder oscillates with large amplitudes, accompanied by the lock-in phenomenon, only in the range over the critical Reynolds number, $\mathrm{Re} = 5{\cdot}6 \times 10^4$–$9{\cdot}2 \times 10^4$, as shown in Figure 5.

Figures 7 and 8 show the response characteristics of the cylinders roughened with the two other kinds of glass beads, of diameter 1 and 0·8 mm, against the Reynolds number Re. For the cases of a natural frequency of 4·10 Hz in Figure 7(a), and 7·38 and 7·82 Hz in Figure 8(a), an unstable region appears in the subcritical regime, and the peak values of amplitudes

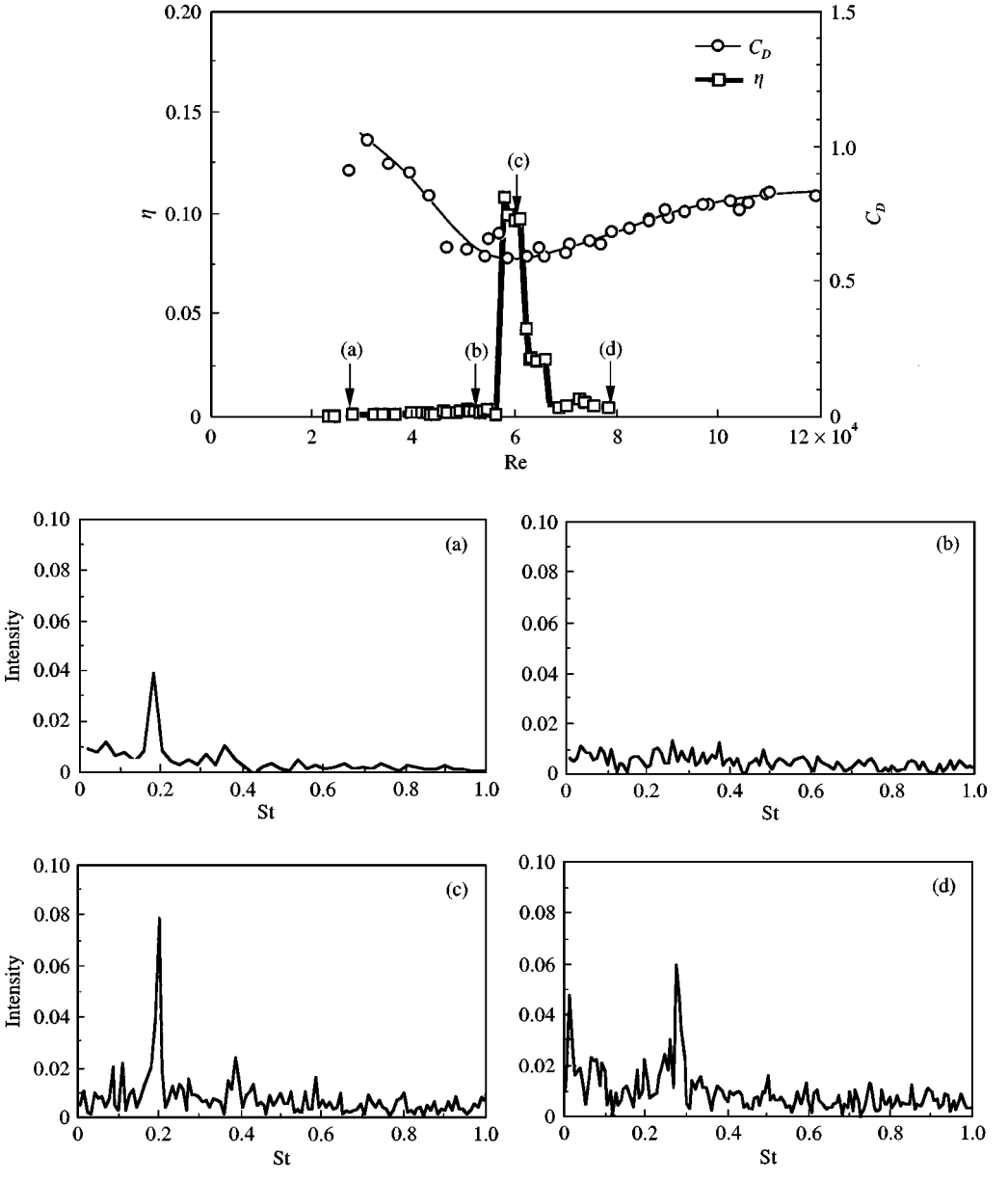

Figure 6. The velocity spectra in the wake for the roughened cylinder of stranded cables with the natural frequency of $f = 5{\cdot}5$ Hz.

η are around 0·16, which agrees with the value of the oscillatory amplitude for a smooth cylinder. In particular, it is found that the response curves of the natural frequency of 7·08 Hz in Figure 7(a) and 9·28 Hz in Figure 8(a) have two amplitude peaks; one below the critical Reynolds number of 5×10^4 and 8×10^4, respectively, and the other over the critical Reynolds numbers. Furthermore, the Strouhal numbers of the wake are different for each natural frequency of cylinder during lock-in oscillation as shown in Figures 7(b) and 8(b).

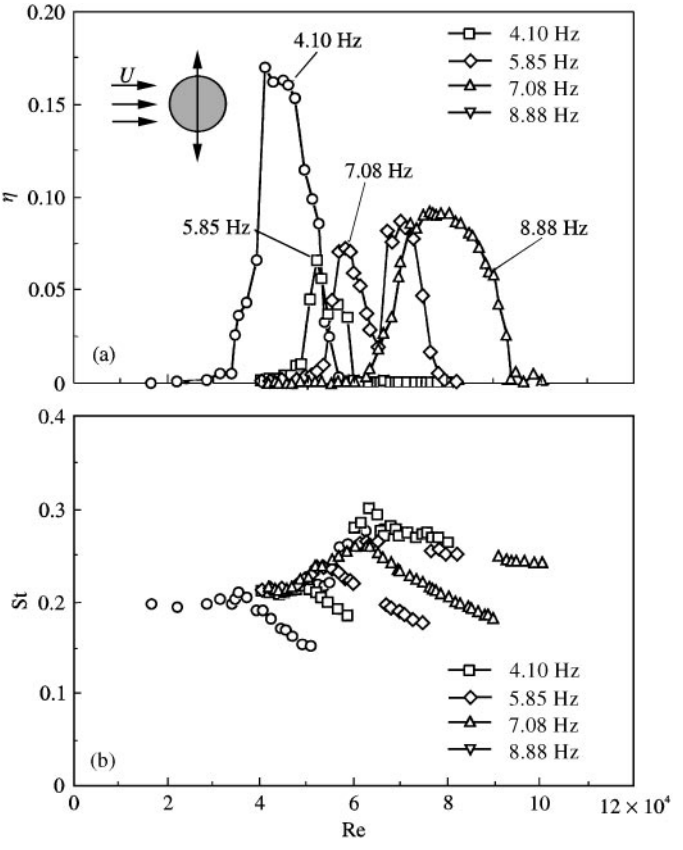

Figure 7. (a) The r.m.s. values, $\eta = a_y/D$ of the displacement response amplitudes, and (b) the Strouhal numbers St of the cylinder roughened with glass beads of 1 mm diameter against the Reynolds number Re; Sc = 6.

The Strouhal number curves of $f = 7{\cdot}08$ Hz [$\diamond$ in Figure 7(b)] and $f = 9{\cdot}28$ Hz [$\triangle$ in Figure 8(b)] are found to be interrupted near the critical Reynolds number since the cylinder oscillation is damped in these regions.

4. CONCLUSIONS

The transverse oscillations of a spring-mounted circular cylinder have been investigated in a wind tunnel over a range of high Reynolds numbers, including the flows near and over the critical Reynolds number. Evenly roughened surfaces made by attaching glass-bead particles and stranded cables have been employed. In the free-oscillation tests, the measured range of reduced velocity is about 1·5 to 8, which includes the critical velocity, and the reduced mass-damping parameter is kept constant at about 6.

The main results can be summarized as follows.

(i) Flows near the critical Reynolds number can be simulated at a relatively low value of wind velocity by using a cylinder with surface roughness.

(ii) The negative damping force seems to be weak around the critical Reynolds number; i.e., the oscillation of the cylinder induced by vortex-excitation can be damped down by a small structural damping near the critical Reynolds number. When the Reynolds number

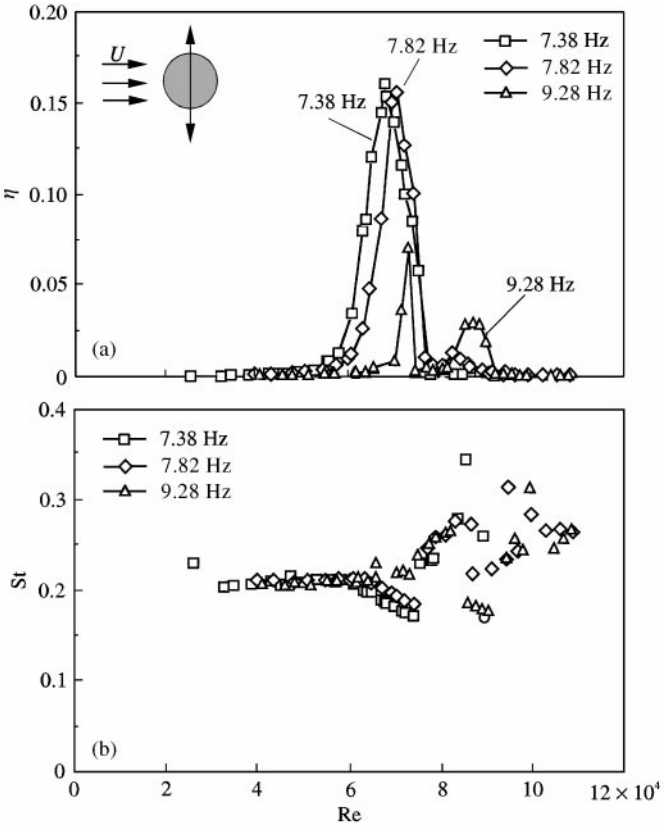

Figure 8. (a) The r.m.s. values, $\eta = a_y/D$ of the displacement response amplitudes, and (b) the Strouhal numbers St of the cylinder roughened with glass beads of a diameter of 0·8 mm against the Reynolds number Re; Sc = 6.

of the flow is over the critical one, the cylinder oscillates with a large amplitude, in a locked-in oscillation.

ACKNOWLEDGEMENTS

One of the authors, A. Okajima, had the privilege of a long and rewarding study under the guidance of the late Prof. Yasuharu Nakamura, whose insightful studies on interaction between fluids and structures have influenced us.

Helpful discussion with Dr M. M. Zdravkovich, University of Salford, U.K. is also gratefully acknowledged.

References

Allen, H. J. & Vincenti, W. G. 1944 Wall interference in a two-dimensional-flow wind tunnel, with consideration of the effect of compressibility. NACA Tech. Report. No. 782, pp. 155–184.

Brika, D. & Laneville, A. 1994 Vortex-induced vibrations of a long flexible circular cylinder. *Journal of Fluid Mechanics* **250,** 481–508.

Feng, C. C. 1968 The measurement of vortex-induced effects in flow past stationary and oscillating circular and D-section cylinders. M.A.Sc. thesis, University of British Columbia, Vancouver, Canada.

King, R., Prosser, M. J. & Johns, D. J. 1973 On vortex excitation of model piles in water. *Journal of Sound and Vibration* **29,** 169–188.

SCRUTON, C. 1963 On the wind-excited oscillations of stacks, towers and masts. *Proceedings of International Conference of Wind Effects on Buildings and Structure*, 798–832. Teddington: Her Majesty's Stationery Office.

WOOTTON, L. R. 1969 The oscillation of large circular stacks in wind. *Proceedings of the Institution of Civil Engineers* **43,** 573–598.

APPENDIX: NOMENCLATURE

a_y	displacement amplitude of an oscillating cylinder in transverse direction
C_D	drag coefficient of a stationary circular cylinder
D	diameter of a circular cylinder
d	diameter of stranded cables for surface roughness
f	natural frequency of oscillating cylinder system
f_w	frequency of fluctuating velocity in the wake
L	span-length of a circular cylinder
M	equivalent mass of a oscillating cylinder system
Re	Reynolds number, equal to UD/v
Sc	reduced mass-damping parameter, Scruton number, equal to $2\delta M/\rho D^2 L$
St	Strouhal number, equal to $f_w D/U$
U	wind velocity
$\bar{U}$	reduced velocity, equal to U/fD
$\bar{U}_{cr}$	the reduced critical velocity, equal to $U/f_w D$
δ	logarithmic damping decrement of oscillating system of a cylinder
η	nondimensional response amplitude of oscillating cylinder in transverse direction, equal to a_y/D
v	kinematic viscosity of air
ρ	air density